J Biomol NMR (2013) 57:47–55
DOI 10.1007/s10858-013-9764-4

ARTICLE

Protein conformational exchange measured by ^{1}H $R_{1\rho}$ relaxation dispersion of methyl groups

Ulrich Weininger · Annica T. Blissing · Janosch Hennig · Alexandra Ahlner · Zhihong Liu · Hans J. Vogel · Mikael Akke · Patrik Lundström

Received: 13 April 2013 / Accepted: 17 July 2013 / Published online: 2 August 2013

Abstract Activated dynamics plays a central role in protein function, where transitions between distinct conformations often underlie the switching between active and inactive states. The characteristic time scales of these transitions typically fall in the microsecond to millisecond range, which is amenable to investigations by NMR relaxation dispersion experiments. Processes at the faster end of this range are more challenging to study, because higher RF field strengths are required to achieve refocusing of the exchanging magnetization. Here we describe a rotating-frame relaxation dispersion experiment for ^{1}H spins in methyl $^{13}CHD_2$ groups, which improves the characterization of fast exchange processes. The influence of ^{1}H–^{1}H rotating-frame nuclear Overhauser effects (ROE) is shown to be negligible, based on a comparison of $R_{1\rho}$ relaxation data acquired with tilt angles of 90° and 35°, in which the ROE is maximal and minimal, respectively, and on samples containing different ^{1}H densities surrounding the monitored methyl groups. The method was applied to ubiquitin and the apo form of calmodulin. We find that ubiquitin does not exhibit any ^{1}H relaxation dispersion of its methyl groups at 10 or 25 °C. By contrast, calmodulin shows significant conformational exchange of the methionine methyl groups in its C-terminal domain, as previously demonstrated by ^{1}H and ^{13}C CPMG experiments. The present $R_{1\rho}$ experiment extends the relaxation dispersion profile towards higher refocusing frequencies, which improves the definition of the exchange correlation time, compared to previous results.

Keywords Relaxation dispersion · Conformational exchange · Rotating-frame relaxation

Introduction

Conformational transitions on the micro- to millisecond time scale are often critical for biological function. A number of studies have shown that transiently populated high-energy states play important roles in enzyme catalysis (Boehr et al. 2006; Cole and Loria 2002; Eisenmesser et al. 2002; Sprangers et al. 2005) or ligand binding by conformational selection (Bruschweiler et al. 2009; Malmendal et al. 1999). Rare transitions between alternative conformations generally lead to modulation of NMR parameters, such as the chemical shift (Gutowsky and Saika 1953) or residual dipolar couplings (Igumenova et al. 2007; Vallurupalli et al. 2007), causing exchange contributions to transverse relaxation rates. Correlation times of biologically relevant exchange processes often fall in the range of milliseconds to microseconds, which can be probed by NMR relaxation dispersion methods, such as the $R_{1\rho}$ (Akke and Palmer 1996; Deverell et al. 1970; James et al. 1977) or Carr-Purcell-Meiboom-Gill (CPMG) experiment

Electronic supplementary material The online version of this article (doi:10.1007/s10858-013-9764-4) contains supplementary material, which is available to authorized users.

U. Weininger · M. Akke (✉)
Department of Biophysical Chemistry, Center for Molecular Protein Science, Lund University, P.O. Box 124, 22100 Lund, Sweden
e-mail: mikael.akke@bpc.liu.se

A. T. Blissing · J. Hennig · A. Ahlner · P. Lundström (✉)
Division of Molecular Biotechnology, Department of Physics, Chemistry and Biology, Linköping University, 58183 Linköping, Sweden
e-mail: patlu@ifm.liu.se

Z. Liu · H. J. Vogel
Department of Biological Sciences, Biochemistry Research Group, University of Calgary, 2500 University Drive NW, Calgary, AB T2N N14, Canada

(Carr and Purcell 1954; Meiboom and Gill 1958) and improved variants of these (Hansen et al. 2008; Igumenova and Palmer 2006; Loria et al. 1999a, b). In favorable cases, relaxation dispersion experiments yield the exchange rate, k_{ex}, the relative populations of the exchanging states, p_i, and the difference in resonance frequency, $\Delta\omega$, between them. To date, experiments have been designed to probe conformational exchange at specific sites in proteins, including the backbone (Akke and Palmer 1996; Hill et al. 2000; Igumenova and Palmer 2006; Ishima et al. 1998, 2004; Ishima and Torchia 2003; Loria et al. 1999a, b; Lundström and Akke 2005a, b; Lundström et al. 2008, 2009a; Mulder and Akke 2003) and side-chain aliphatic (Hansen et al. 2012; Lundström et al. 2009b), carbonyl/carboxyl (Hansen and Kay 2011; Paquin et al. 2008), side-chain amide (Mulder et al. 2000) and aromatic (Weininger et al. 2012b) groups. Methyl groups take a special place because they are ideal probes of protein interactions and dynamics due to their favorable NMR relaxation properties leading to sharp signals in ^{1}H and ^{13}C NMR spectra. Furthermore, methyl-bearing amino-acid residues are prevalent in proteins, where they make up approximately 50 % of the hydrophobic core and often are present in crevices or surface regions implicated in protein–ligand or protein–protein interactions (Kay et al. 1998; Lee et al. 2000). For these reasons, a number of relaxation dispersion experiments have been developed previously for studying methyl group dynamics by ^{13}C CPMG or $R_{1\rho}$ approaches (Brath et al. 2006; Ishima et al. 1999; Lundström et al. 2007; Mulder et al. 2002; Skrynnikov et al. 2001; Weininger et al. 2012a) or ^{1}H CPMG (Baldwin et al. 2010; Otten et al. 2010b; Weininger et al. 2012a). Compared to CPMG-based experiments, $R_{1\rho}$ experiments generally can achieve higher refocusing frequencies, which are limited in the former case by the duty cycle of the CPMG train, $\omega_{CP} = \pi/\tau_{CP}$, where τ_{CP} is the delay between the high-power 180° pulses. In the case of $R_{1\rho}$ experiments, ^{1}H is an advantageous nucleus since the refocusing frequency scales with the gyromagnetic ratio and the RF field amplitude, $\omega_1 = \gamma B_1$. These considerations provide a strong impetus for the development of ^{1}H $R_{1\rho}$ pulse sequences. Here we present $R_{1\rho}$ pulse sequences for ^{1}H spins in methyl groups, designed to suit $^{13}CHD_2$ isotopomers that are either isolated or located in spin systems containing neighboring ^{13}C nuclei. Further we show that in highly deuterated background $R_{1\rho}$ measurements are not affected by Overhauser effects (ROE).

Materials and methods

Protein samples

Uniformly ^{13}C/^{15}N and partially ^{2}H labeled human ubiquitin was purchased from ASLA Biotech. The protein was expressed in M9 medium containing 99.9 % D_2O and supplemented with protonated ^{13}C-glucose and $^{15}NH_4Cl$. Calmodulin was expressed and purified as described previously using M9 minimal media containing 99.9 % D_2O, 0.5 g/l $^{15}NH_4Cl$, 4 g/l non-isotope enriched glucose and 100 mg/l $^{12}C^{\alpha}H$–($^{12}CD_2$)$_2$–S–$^{13}CHD_2$ methionine (Gifford et al. 2011; Weininger et al. 2012a).

NMR spectroscopy

All NMR experiments were conducted using Varian DirectDrive 500 MHz and Varian Inova 600 MHz and 900 MHz spectrometers. Ubiquitin data was recorded on a 1.2 mM sample in 50 mM KP_i pH 6.9, 50 μM NaN_3, 10 % D_2O at 25 °C with the constant time version of the pulse sequence described in Fig. 1. $R_{1\rho}$ rate constants were measured at 600 MHz at a nominal tilt angle of 90° at twelve different spin-lock fields ranging from $\omega_1 = 4{,}122$ to 67,419 s^{-1}. The carrier position was 0.75 ppm, corresponding to the middle of the Ile, Leu and Val region of the spectrum. The experiment was repeated with the same spin-lock fields but with carrier positions equivalent to nominal tilt angles of 35°. Apo calmodulin data was recorded on a 1 mM sample in 20 mM Tris pH 6.5, 7 % D_2O at 25 °C using the non-constant time version of the pulse sequence. Experiments were performed at 500 MHz with nominal tilt-angles of 90° and 35° and nine different spin-lock fields ranging from $\omega_1 = 1{,}608$ to 50,347 s^{-1}. The experiments with nominal tilt-angles of 90° were repeated at 900 MHz for twelve different spin-lock fields ranging from $\omega_1 = 1{,}891$ to 37,762 s^{-1}.

Data analysis

All data was processed in NMRpipe (Delaglio et al. 1995) and visualized in NMRview (Johnson and Blevins 1994) and Sparky (Goddard and Kneller). Peaks were integrated and the rotating-frame relaxation rate constants ($R_{1\rho}$) were extracted from fits to exponential functions or linear two-point approximations of these. In the fast exchange limit the rotating-frame relaxation rate constant is given by

$$R_{1\rho}(\omega_{eff}, \theta) = \cos^2\theta R_1 + \sin^2\theta R_2^0 + \sin^2\theta \frac{\phi_{ex} k_{ex}}{k_{ex}^2 + \omega_{eff}^2} \quad (1)$$

where R_1 and R_2^0 are the longitudinal and exchange-free transverse relaxation rate constants, respectively, θ is the tilt angle, given by $\tan\theta = B_1/\Omega$, where B_1 is the strength of the spin-lock field and Ω is the resonance offset from the carrier position of the spin-lock field, ω_{eff} is the effective field given by $\omega_{eff} = \left(B_1^2 + \Omega^2\right)^{0.5}$, ϕ_{ex} is the product of the relative populations of the exchanging states and the square of their difference in resonance frequencies and k_{ex} is the

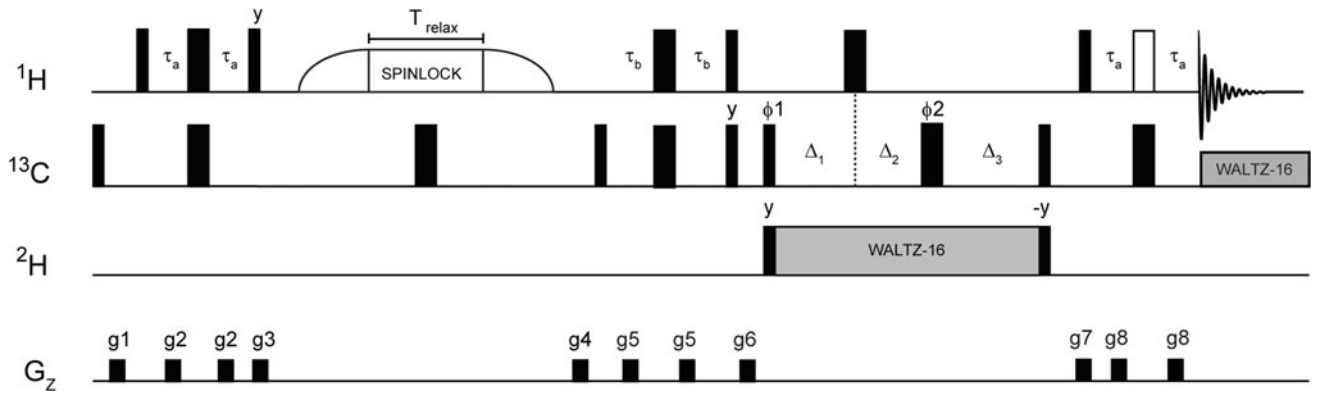

Fig. 1 Pulse sequence for measurements of ^{1}H methyl $R_{1\rho}$ rates. Filled narrow (wide) rectangles depict 90° (180°) pulses applied at the highest possible power. The unfilled rectangle represents a 3-9-19 binomial pulse. The phase of all pulses is x unless otherwise noted. The delays are $\tau_a = 1.67$ ms, $\tau_b = 2.0$ ms, $T_c = 14.3$ ms, $\Delta_1 = \tau_b + t_1/2$, $\Delta_2 = T_c - \tau_b$, $\Delta_3 = T_c - t_1/2$. During ^{13}C evolution, ^{2}H is decoupled by a WALTZ-16 sequence of field strength $\gamma B_1/2\pi = 920$ Hz centered at the methyl region. The decoupling is applied along the *x*-axis and flanked by 90° pulses applied at the same field strength. ^{13}C decoupling during acquisition is achieved by WALTZ-16 applied at a field strength of $\gamma B_1/2\pi = 1{,}880$ Hz at 500 MHz and scaled appropriately for experiments performed at other static magnetic field strengths. The spin-lock relaxation delay is flanked by 8 ms tan/tanh adiabatic pulses that align the magnetization with the effective field and return it to the *z*-axis, respectively. The adiabatic sweep is initiated 25 kHz downfield or upfield of the spin-lock frequency (software to generate the adiabatic pulses is available upon request). Gradient strengths in G/cm (durations in ms) are: g1 = 5,000 (0.3), g2 = 6,000 (1.0), g3 = 5,000 (0.3), g4 = −3,000 (0.23), g5 = −8,500 (0.3), g6 = 5,500, g7 = 11,000 (1), g8 = 19,000 (0.9). The phase cycle is $\phi1 = \{x, -x\}$, $\phi2 = \{x, x, y, y, -x, -x, -y, -y\}$ and the receiver phase is $\{x, -x, y, -y\}$. Quadrature detection in t_1 is achieved by incrementing $\phi1$ by $\pi/2$. For every increment $\phi1$ and the receiver are incremented by π. For samples with isolated methyl ^{13}C groups non-constant time evolution in t_1 is achieved by setting $\Delta_1 = \tau_b + t_1/2$, $\Delta_2 = t_1/2$, $\Delta_3 = \tau_b$

exchange rate. Here, we fitted the $R_{1\rho}$ rate constants to models that either included or excluded fast chemical exchange, assuming a constant tilt angle for all effective fields, i.e.

$$R_{1\rho}(\omega_{eff}, \theta) = R^0_{1\rho} \tag{2}$$

$$R_{1\rho}(\omega_{eff}, \theta) = R^0_{1\rho} + \sin^2\theta \frac{\phi_{ex} k_{ex}}{k^2_{ex} + \omega^2_{eff}} \tag{3}$$

where $R^0_{1\rho} = \cos^2\theta\, R_1 + \sin^2\theta\, R^0_2$ is the rotating-frame relaxation rate in the limit of an infinitely strong effective field. The ubiquitin data was fitted to Eq. 2. Only data points with tilt angles $85° < \theta < 95°$ and $34° < \theta < 36°$, respectively, were considered. The data for CaM was fitted to Eqs. 2 and 3 on a residue-by-residue basis, using data points with tilt angles $82° < \theta < 98°$ and $33° < \theta < 39°$. This slightly higher variance in tilt angles in CaM is compensated by lower differences between R_1 and R_2. Residues for which the chemical exchange model was significant were subsequently refitted to Eq. 3 using a global exchange rate. The uncertainties in the fitted parameters were estimated by Monte Carlo simulations (Press et al. 1988).

Results

The pulse sequence for measurement of methyl proton $R_{1\rho}$ rate constants is shown in Fig. 1. Following Skrynnikov and coworkers we applied the spin-lock to density operator terms corresponding to anti-phase coherences and longitudinal two-spin order (Eichmuller and Skrynnikov 2005). This approach has the advantage that these operators relax to zero, because they do not correspond to equilibrium magnetization. The increased relaxation rate due to external longitudinal relaxation contributions from ^{13}C is negligible for methyl groups in highly deuterated samples. The element following the relaxation delay is used to select for the desired $^{13}CHD_2$ isotopomer (Liao and Tugarinov 2011), which leads to considerable spectral simplification for samples containing a mixture of $^{13}CH_3$ and $^{13}CH_2D$ and $^{13}CHD_2$ and $^{13}CD_3$ isotopomers. In large proteins, cross-correlated dipolar relaxation involving multiple ^{1}H–^{13}C spin pairs reduces the efficacy of the multiplicity filter that rejects the $^{13}CH_3$ isotopomer (Liao and Tugarinov 2011), but for small proteins the strategy works well, as demonstrated here for ubiquitin ($M_w = 8{,}565$ Da) at 25 °C. Also, a judicious choice of deuteration level during protein expression reduces the relative amount of the $^{13}CH_3$ isotopomer (Otten et al. 2010a).

Alignment of the magnetization with the effective field and its subsequent return to the *z*-axis was achieved by adiabatic ramps, where the phase and amplitude are modulated with a tangent and a hyperbolic tangent, respectively. Relatively long ramps of 8 ms were needed to get satisfactory alignment at weak spin-lock field strengths ($\omega_1 < 3{,}000$ s^{-1}). An alternative way of achieving good alignment at low spin-lock field strengths is by means of

chemical shift precession (Akke and Palmer 1996; Hansen and Kay 2007), but since this approach fails for the largest spin-lock fields needed here it was not used. The evolution period in the indirect dimension can be implemented either as constant time for uniformly ^{13}C labeled samples, or as non-constant time for samples with isolated ^{13}C labeled methyl groups.

We applied the ^{1}H methyl $R_{1\rho}$ experiment to measure fast exchange dynamics on the methyl groups in a uniformly ^{13}C and partially (60 %) ^{2}H labeled sample of ubiquitin, as well as on methionine methyl groups in a specifically (100 %) $^{12}C^{\alpha}H$–($^{12}CD_2$)$_2$–S–$^{13}CHD_2$ labeled and partially deuterated (60 %) sample of calmodulin (CaM). The experiments on CaM serve as a benchmark to validate the present ^{1}H methyl $R_{1\rho}$ method against previous results obtained using ^{1}H and ^{13}C CPMG experiments (Weininger et al. 2012a), while the ubiquitin experiments illustrate the implementation of our method in the context of uniformly ^{13}C labeled samples.

Artifact-free dispersions can be measured at 90° tilt angles for partially deuterated samples

In the spin-diffusion limit, dipolar cross relaxation due to the ROE is exactly canceled by cross relaxation due to the NOE at a tilt angle close to 35°. Unfortunately this choice of tilt angle leads to reduced sensitivity to chemical exchange by a factor three due to the reduced projection of the magnetization onto the transverse plane, as can be seen for Eq. 1. It is thus advantageous to identify experimental conditions for which tilt angles of 90° can be used. We have previously shown that partial deuteration is effective for reducing the ROE in amide proton $R_{1\rho}$ relaxation dispersion experiments (Lundström and Akke 2005b). Here we tested this approach in the context of the methyl proton $R_{1\rho}$ experiment by applying on-resonance spin-locks (90° tilt angle) to a uniformly ^{13}C and partially ^{2}H labeled sample of ubiquitin at 25 °C.

Palmer and coworkers have previously published ^{15}N $R_{1\rho}$ relaxation dispersion data on ubiquitin, showing chemical exchange for Ile23, Asn25, Thr55, and Val70 with a rate constant of 25,000 s^{-1} at 7 °C (Massi et al. 2005). Assuming that the exchange rate doubles if the temperature is increased by 10 °C, we would expect an exchange rate of almost 100,000 s^{-1} at 25 °C. Consequently, the exchange contribution to transverse relaxation should be reduced by almost a factor of four and essentially flat dispersion profiles should thus be expected for the great majority of methyl groups in ubiquitin.

We were able to analyze data for 37 out of the 50 methyl groups of ubiquitin. The remaining ones had to be excluded due to severe spectral overlap. Figure 2 shows examples of dispersions for ubiquitin recorded with nominal tilt angles of 90° and 35°. Clearly, these data are well represented by a model that excludes chemical exchange. The average root-mean-square-deviation (RMSD) between the data points and the fitted lines is 0.25 ± 0.15 s^{-1} for a tilt angle of 90° and 0.24 ± 0.16 s^{-1} for a tilt angle of 35° (see SI Fig. 1 for data on all residues) however, data for some methyl groups are more scattered than those shown in Fig. 2. The majority of cases of large RMSDs can be explained by partial spectral overlap or weaker signal intensities, the latter of which often occur for Ala or Thr residues because of a greater fraction of unwanted isotopomers for these residue types. If the Ala and Thr residues are excluded then the average RMSDs drop to 0.19 ± 0.07 s^{-1} and 0.18 ± 0.08 s^{-1} for data at tilt angles of 90° and 35°, respectively. Taking all residues into account, we find that the datasets from the two tilt angles are not qualitatively different and there is no indication of chemical exchange. These results indicate that the data recorded with a tilt angle of 90° are free from ROE artifacts, since similar profiles result for data acquired at either tilt angle. To further verify this conclusion, we back-calculated $R_{1\rho}$ at a tilt angle of 35° from Eq. 1, taking as input data R_1 (measured for $2C_zH_z$ in a separate experiment) and $R_{1\rho}$ measured at a tilt angle of 90°. The back-calculated values agree very well with the measured ones (see SI Fig. 1) and, importantly, there is no systematic bias. It should be noted that only protons attached to ^{13}C can contribute to ROE artifacts since magnetization originating on other protons is dephased prior to the spinlock period.

In fitting the relaxation dispersion curves, we employed the approximation that the tilt-angle was constant for all effective fields (at each nominal tilt-angle). This is a reasonable approximation as long as the variation in tilt-angle is small. For example, if the tilt-angle varies in the range 85–95° with $R_1 = 1.7$ s^{-1} and $R_2^0 = 3.6$ s^{-1}, then $R_{1\rho}$ varies between 3.59 and 3.60 s^{-1}, which is well within the experimental error. At other tilt angles the analysis may require more precise values of θ. In the range 34–36°, $R_{1\rho}$ varies between 2.29 and 2.36 s^{-1}, with $R_{1\rho} = 2.33$ s^{-1} at $\theta = 35°$. It is possible to minimize the chemical-shift dependence of θ by averaging results from experiments acquired with positive and negative tilt angles, e.g. $\theta = \pm 35°$ (Eichmuller and Skrynnikov 2005; Schleucher et al. 1995). However, for the purposes of the present validation, the approximative approach is sufficient.

We were also interested in whether there were microsecond dynamics at lower temperatures and therefore we repeated the experiments at 10 °C (data not shown). In contrast with previous results for ^{15}N at 7 °C (Massi et al. 2005), we did not detect any microsecond dynamics at this temperature either. We emphasize that the absence of detectable exchange contributions to the rotating-frame relaxation experiment for the methyl protons of ubiquitin is not in disagreement with previous results, but merely

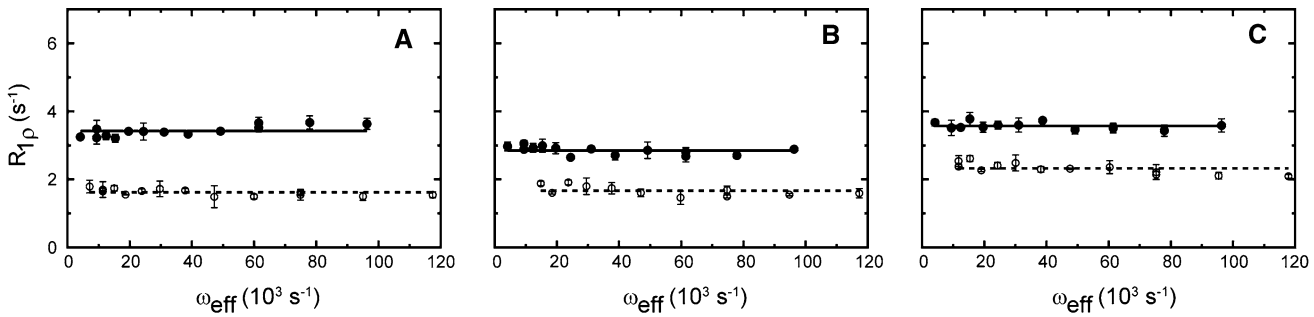

Fig. 2 Representative methyl ^{1}H $R_{1\rho}$ relaxation dispersion profiles for ubiquitin. Data is shown for **a** Ile13 Hδ1, **b** Leu67 Hδ2 and **c** Val70 Hγ2. *Circles* represent measured $R_{1\rho}$ rate constants and lines indicate fits to exchange-free models for nominal tilt angles of 90° (*filled circles*, *solid lines*) and 35° (*open circles*, *dashed lines*). The pairwise RMSDs between the fitted lines and the experimental data obtained at $\theta = 90°$ (35°) are 0.15 (0.096), 0.12 (0.15) and 0.096 (0.15) for panels **a**, **b**, and **c**, respectively

demonstrates that the chemical shifts of different nuclei might be modulated to different extents by a given dynamical process.

Fast exchange in apo-CaM measured at 35° and 90° tilt angles

In order to further investigate possible NOE/ROE effects in ^{1}H methyl $R_{1\rho}$ dispersion experiments, we acquired data at 11.7 T (Fig. 3 and SI Fig. 2) on the methionine methyl groups of apo-CaM at tilt angles close to 35° (33–39°), where ROE and NOE effects cancel, and close to 90° (82–98°), where the sensitivity to chemical exchange and the ROE are both maximal. Met51 does not show any significant relaxation dispersion amplitude, $R_{1\rho}(\omega_{\text{eff}} \rightarrow 0) - R_{1\rho}(\omega_{\text{eff}} \rightarrow \infty) < 0.5\ \text{s}^{-1}$, indicating there are no or very minor contributions from conformational exchange. By contrast, Met124 and Met144 clearly show dispersion profiles indicative of exchange. These results are in keeping with previous CPMG dispersion experiments (Weininger et al. 2012a). As expected, the exchange contributions to $R_{1\rho}$ is more pronounced at 90° tilt angles (Fig. 3d, f), demonstrating the advantage of performing the experiment under these conditions. Individual fits of the ^{1}H methyl $R_{1\rho}$ dispersions at 35° and 90° tilt angles resulted in identical exchange rates within experimental error: 6,500 ± 1,000 s^{-1} (35°) and 7,000 ± 1,000 s^{-1} (90°) for Met124; and 5,100 ± 900 s^{-1} (35°) and 5,800 ± 400 s^{-1} (90°) for Met144. These results verify that NOE/ROE effects are insignificant in highly deuterated samples, making it possible to study exchange processes at their maximal impact at 90° tilt angles.

Global exchange process in the C-terminal domain of apo CaM

Having ensured that ROEs do not affect exchange measurements at 90° tilt angles, we investigated the global exchange process in the C-terminal domain under these conditions at two static magnetic fields (11.7 T and 21.1 T). While the N-terminal domain shows no exchange, in agreement with previous studies (Weininger et al. 2012a), the exchange of all four methionine residues in the C-terminal domain (SI Fig. 3) could be analyzed globally, resulting in an exchange rate of 6,600 ± 100 s^{-1}. This rate is slightly higher than the previously reported rate of 4,800 ± 100 s^{-1}, determined using ^{1}H methyl CPMG relaxation dispersion (Weininger et al. 2012a). This discrepancy might be expected, because the rate is on the edge of what the CPMG method is capable of characterizing, since the exchange contribution is not completely quenched even at the highest achievable effective fields. Unless special approaches are used, there is a risk that the CPMG method yields slightly underestimated rates of fast exchange processes (Vallurupalli et al. 2011). This observation nicely demonstrates the advantage of the ^{1}H methyl $R_{1\rho}$ experiment for studying fast processes with high precision. However, the CPMG dispersions can be refitted using the value of k_{ex} determined by $R_{1\rho}$ as a fixed parameter to yield results that are virtually indistinguishable from the free fit. Indeed, the reduced χ^2 from the least-squares optimization of the CPMG data only increased from 1.96 to 2.50 when k_{ex} was kept fixed. Examples for two residues in the C-terminal domain are shown in Fig. 4. It is clear that they are well fitted by a global process and that the CPMG data are compatible with the exchange rate constant extracted from $R_{1\rho}$ measurements.

We used the re-fitted CPMG data to calculate ϕ_{ex} for the individual methionine methyl groups and compare with ϕ_{ex} obtained from $R_{1\rho}$ dispersions. The correlation is shown in Fig. 5, together with the line corresponding to perfect correlation and a slope of unity. The actual slope is 1.12 ± 0.1, showing the excellent correlation between data acquired using the two different approaches.

A question that arises concerns the practical limit when CPMG relaxation dispersion experiments fail and one must

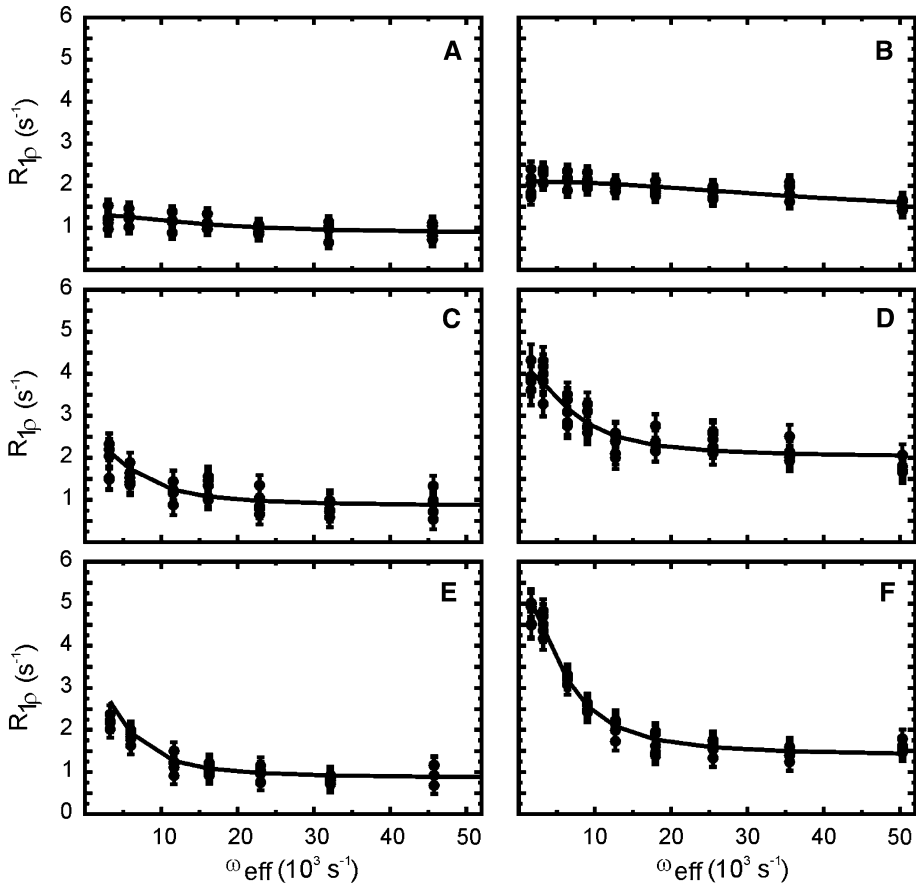

Fig. 3 Representative ^{1}H methyl $R_{1\rho}$ relaxation dispersion profiles at nominal tilt angles of 35° (**a**, **c**, **e**) and 90° (**b**, **d**, **f**). Data were acquired on a 1 mM sample of apo-CaM specifically labeled with $^{12}C^{\alpha}H$–($^{12}CD_2$)$_2$–S–$^{13}CHD_2$ Met at a static magnetic field strength of 11.7 T and a temperature of 25 °C. All experiments were repeated five times at each effective field. For Met51 (**a**, **b**) no exchange could be detected. Exchange processes in Met124 (**c**, **d**) and Met144 (**e**, **f**) were analyzed by individual fits (*solid lines*) to a two-state model resulting in exchange rates k_{ex} of 6,500 ± 1,000 s^{-1} (Met124, 35°), 7,000 ± 1,000 s^{-1} (Met124, 90°), 5,100 ± 900 s^{-1} (Met144, 35°) and 5,800 ± 400 (Met144, 90°)

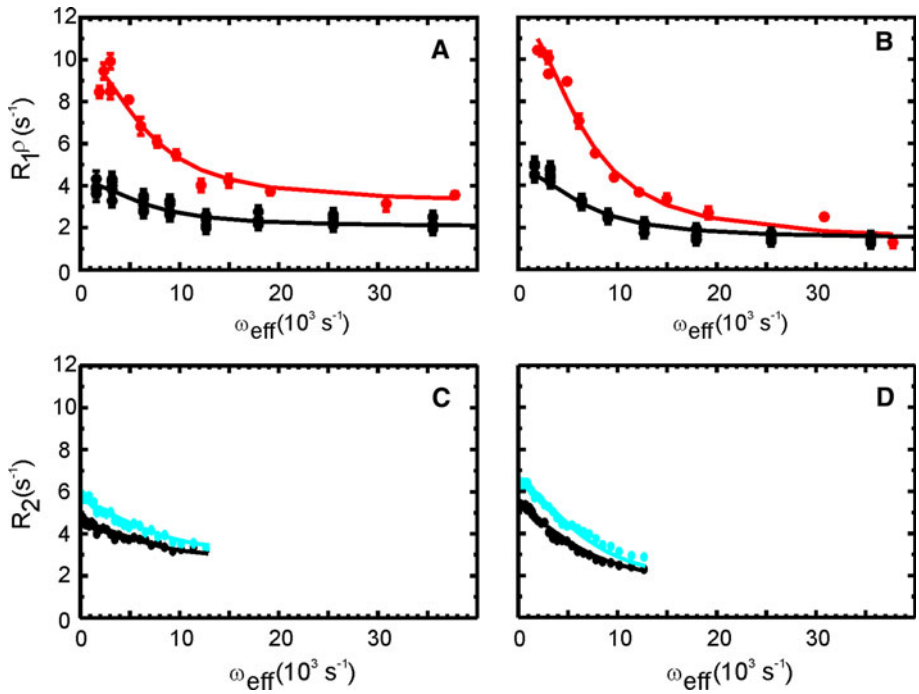

Fig. 4 ^{1}H methyl relaxation dispersion profiles of Met124 (**a**, **c**) and Met144 (**b**, **d**) of apo-CaM. (**a**, **b**) $R_{1\rho}$ relaxation dispersion profiles at tilt angles close to 90° and static magnetic field strengths of 11.7 T (*black*) and 21.1 T (*red*) at 25 °C. A simultaneous fit of a global two-state model to the data at both static magnetic fields for each residue (*solid lines*) results in k_{ex} = 6,600 ± 100 s^{-1}. (**c**, **d**) Previously recorded CPMG dispersions re-fitted with k_{ex} fixed to 6,600 s^{-1}; data and fits (*solid lines*) at shown for 11.7 T (*black*) and 14.1 T (*cyan*)

resort to $R_{1\rho}$ experiments. There is no unique answer to this question since the limit depends on hardware specifications and on the relative sensitivity of the two experiments. The above comparison between our present results on calmodulin and previous CPMG data (Weininger et al. 2012a) provides an indication that the limit is around 5,000 s^{-1},

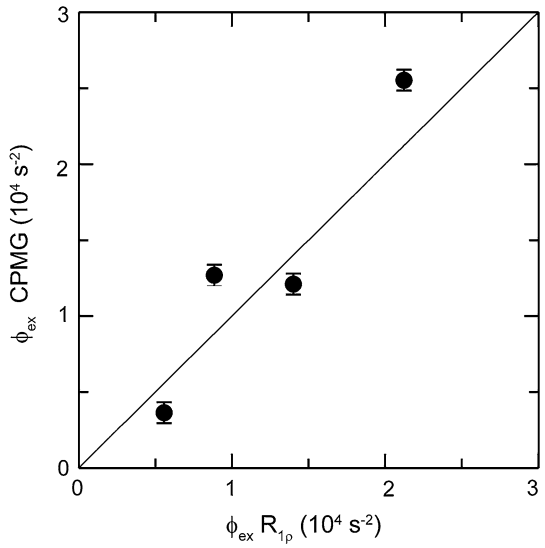

Fig. 5 Correlation of ϕ_{ex} values from ^{1}H methyl $R_{1\rho}$ fitted to a global exchange rate and ϕ_{ex} from ^{1}H methyl CPMG fitted using the same exchange rate as in the $R_{1\rho}$ experiment. Errors of ϕ_{ex} obtained from $R_{1\rho}$ are within the symbol sizes. The line represents the function y = x, expected for perfect correlation of the data sets

given the experimental conditions used in our studies. Furthermore, considering that the calmodulin CPMG data cover the relaxation dispersion curve down to 22 % of the total dispersion amplitude using a maximum $\omega_{CP}/2\pi$ of 2,000 Hz, we expect that the same level of coverage can be obtained using the present range of $R_{1\rho}$ field strengths (up to 10,729 Hz) for an exchange rate of 35,800 s^{-1}. Of course, these numbers in no way represent an absolute upper limit and especially using modern cryo-probes that tolerate more power it is possible to measure significantly faster processes (>100,000 s^{-1}) using on-resonance $R_{1\rho}$ experiments as discussed by Griesinger and co-workers (Ban et al. 2012).

Since the dispersion step is given by $\phi_{ex}/k_{ex} = p_a(1-p_a)\Delta\omega^2/k_{ex}$ for two-site exchange in the fast exchange limit, it is clear that increasingly larger chemical shift differences between the exchanging states are needed to get sizable exchange contributions as the exchange rates are getting faster. In the case of methyl groups in medium-sized proteins, a dispersion step of 2 s^{-1} provides sufficient amplitude to yield high-quality dispersion profiles suitable for model fitting. Given that the standard deviation of methyl proton chemical shifts deposited in the Biological Magnetic Resonance Data Bank (Ulrich et al. 2008) ranges between 0.26 and 0.29 ppm for Ile-Leu-Val and is 0.22 ppm for Thr and 0.46 ppm for Met, we expect that conformational exchange can be measured for fast exchange rates. For example, given an exchange rate of 100,000 s^{-1} and equal populations of the two states, $\phi_{ex}/k_{ex} = 2$ s^{-1} results from a chemical shift difference of 0.28 ppm at a static magnetic field of 11.7 T; alternatively, if the minor state is populated to 10 %, then a static magnetic field strength of 18.8 T yields comparable results. For increasingly skewed populations or faster exchange rates, larger chemical shift differences and/or higher static magnetic fields are required.

In conclusion, we have developed ^{1}H $R_{1\rho}$ experiments for $^{13}CHD_2$ methyl groups. Two variants of the pulse sequence are available for use with either uniformly ^{13}C-labeled proteins and partially deuterated proteins, or for isolated $^{13}CHD_2$ methyl groups, e.g. for selectively labeled methionine, isoleucine, leucine and valine residues (Baldwin et al. 2010; Goto et al. 1999; Ollerenshaw et al. 2005; Weininger et al. 2012a). Furthermore, the experiment is equally suitable for samples labeled specifically with CHD_2 groups or a mixture of CHD_2, CH_2D and CH_3 groups. The experiment complements previously described approaches and allows characterization of exchange processes on the order of 50,000 s^{-1} using on-resonance spin-lock fields. We have shown that the experiment can be used to characterize microsecond dynamics between conformers within the folded ensemble. Additional applications include studies of ultrafast folding-unfolding dynamics and transient ligand-binding events.

Acknowledgments This research was supported by the Swedish Research Council (621-2010-4912; 822-2005-2915; 621-2012-5136), the Göran Gustafsson Foundation for Research in Natural Sciences and Medicine, and the Knut and Alice Wallenberg Foundation. UW was supported by an EMBO long-term fellowship and JH was supported by a Forum Scientium Award. HJV holds a Scientist award from Alberta Innovates Health Solutions. We thank SWEDSTRUCT for access to the 900 MHz spectrometer at the Swedish NMR Centre.

References

Akke M, Palmer AG (1996) Monitoring macromolecular motions on microsecond–millisecond time scales by $R_{1\rho}$–R_1 constant-relaxation-time NMR spectroscopy. J Am Chem Soc 118:911–912

Baldwin AJ, Religa TL, Hansen DF, Bouvignies G, Kay LE (2010) $^{13}CHD_2$ methyl group probes of millisecond time scale exchange in proteins by ^{1}H relaxation dispersion: an application to proteasome gating residue dynamics. J Am Chem Soc 132:10992–10995

Ban D, Gossert AD, Giller K, Becker S, Griesinger C, Lee D (2012) Exceeding the limit of dynamics studies on biomolecules using high spin-lock field strengths with a cryogenically cooled probehead. J Magn Reson 221:1–4

Boehr DD, McElheny D, Dyson HJ, Wright PE (2006) The dynamic energy landscape of dihydrofolate reductase catalysis. Science 313:1638–1642

Brath U, Akke M, Yang D, Kay LE, Mulder FAA (2006) Functional dynamics of human FKBP12 revealed by methyl ^{13}C rotating frame relaxation dispersion NMR spectroscopy. J Am Chem Soc 128:5718–5727

Bruschweiler S, Schanda P, Kloiber K, Brutscher B, Kontaxis G, Konrat R, Tollinger M (2009) Direct observation of the dynamic

process underlying allosteric signal transmission. J Am Chem Soc 131:3063–3068
Carr HY, Purcell EM (1954) Effects of diffusion on free precession in nuclear magnetic resonance experiments. Phys Rev 94:630–638
Cole R, Loria JP (2002) Evidence for flexibility in the function of ribonuclease A. Biochemistry 41:6072–6081
Delaglio F, Grzesiek S, Vuister GW, Zhu G, Pfeifer J, Bax A (1995) NMRPipe: a multidimensional spectral processing system based on UNIX pipes. J Biomol NMR 6:277–293
Deverell C, Morgan RE, Strange JH (1970) Studies of chemical exchange by nuclear magnetization relaxation in the rotating frame. Mol Phys 18:553–559
Eichmuller C, Skrynnikov NR (2005) A new amide proton $R_{1\rho}$ experiment permits accurate characterization of microsecond time-scale conformational exchange. J Biomol NMR 32:281–293
Eisenmesser EZ, Bosco DA, Akke M, Kern D (2002) Enzyme dynamics during catalysis. Science 295:1520–1523
Gifford JL, Ishida H, Vogel HJ (2011) Fast methionine-based solution structure determination of calcium–calmodulin complexes. J Biomol NMR 50:71–81
Goddard TD, Kneller DG SPARKY 3. University of California, San Francisco
Goto NK, Gardner KH, Mueller GA, Willis RC, Kay LE (1999) A robust and cost-effective method for the production of Val, Leu, Ile (δ1) methyl-protonated ^{15}N–, ^{13}C–, ^{2}H-labeled proteins. J Biomol NMR 13:369–374
Gutowsky HS, Saika A (1953) Dissociation, chemical exchange, and the proton magnetic resonance in some aqueous electrolytes. J Chem Phys 21:1688–1694
Hansen DF, Kay LE (2007) Improved magnetization alignment schemes for spin-lock relaxation experiments. J Biomol NMR 37:245–255
Hansen AL, Kay LE (2011) Quantifying millisecond time-scale exchange in proteins by CPMG relaxation dispersion NMR spectroscopy of side-chain carbonyl groups. J Biomol NMR 50:347–355
Hansen DF, Vallurupalli P, Kay LE (2008) An improved ^{15}N relaxation dispersion experiment for the measurement of millisecond time-scale dynamics in proteins. J Phys Chem B 112:5898–5904
Hansen AL, Lundström P, Velyvis A, Kay LE (2012) Quantifying millisecond exchange dynamics in proteins by CPMG Relaxation dispersion NMR using side-chain H-1 Probes. J Am Chem Soc 134:3178–3189
Hill RB, Bracken C, DeGrado WF, Palmer AG (2000) Molecular motions and protein folding: characterization of the backbone dynamics and folding equilibrium of alpha D-2 using C-13 NMR spin relaxation. J Am Chem Soc 122:11610–11619
Igumenova TI, Palmer AG (2006) Off-resonance TROSY-selected $R_{1\rho}$ experiment with improved sensitivity for medium- and high-molecular-weight proteins. J Am Chem Soc 128:8110–8111
Igumenova TI, Brath U, Akke M, Palmer AG (2007) Characterization of chemical exchange using residual dipolar coupling. J Am Chem Soc 129:13396–13397
Ishima R, Torchia DA (2003) Extending the range of amide proton relaxation dispersion experiments in proteins using a constant-time relaxation-compensated CPMG approach. J Biomol NMR 25:243–248
Ishima R, Wingfield PT, Stahl SJ, Kaufman JD, Torchia DA (1998) Using amide ^{1}H and ^{15}N transverse relaxation to detect millisecond time-scale motions in perdeuterated proteins: application to HIV-1 protease. J Am Chem Soc 120:10534–10542
Ishima R, Louis JM, Torchia DA (1999) Transverse ^{13}C relaxation of CHD_2 methyl isotopomers to detect slow conformational changes of protein side chains. J Am Chem Soc 121: 11589–11590
Ishima R, Baber J, Louis JM, Torchia DA (2004) Carbonyl carbon transverse relaxation dispersion measurements and ms–μs time-scale motion in a protein hydrogen bond network. J Biomol NMR 29:187–198
James TL, Matson GB, Kuntz ID, Fisher RW (1977) Rotating frame spin-lattice relaxation in the presence of an off-resonance radio frequency field. Investigation of intermediate molecular motions. J Magn Reson 28:417–426
Johnson BA, Blevins RA (1994) NMRView: a computer program for the visualization and analysis of NMR data. J Biomol NMR 4:603–614
Kay LE, Muhandiram DR, Wolf G, Shoelson SE, Forman-Kay JD (1998) Correlation between binding and dynamics at SH2 domain interfaces. Nat Struct Biol 5:156–163
Lee AL, Kinnear SA, Wand AJ (2000) Redistribution and loss of side chain entropy upon formation of a calmodulin-peptide complex. Nat Struct Biol 7:72–77
Liao XL, Tugarinov V (2011) Selective detection of CHD_2-^{13}C signals from a mixture of CH_3-^{13}C/CH_2D-^{13}C/CHD_2-^{13}C methyl isotopomers in proteins. J Magn Reson 209:101–107
Loria JP, Rance M, Palmer AG (1999a) A relaxation-compensated Carr-Purcell-Meiboom-Gill sequence for characterizing chemical exchange by NMR spectroscopy. J Am Chem Soc 121: 2331–2332
Loria JP, Rance M, Palmer AG (1999b) A TROSY CPMG sequence for characterizing chemical exchange in large proteins. J Biomol NMR 15:151–155
Lundström P, Akke M (2005a) Microsecond protein dynamics measured by rotating-frame $^{13}C^{a}$ spin relaxation. Chem Bio Chem 6:1685–1692
Lundström P, Akke M (2005b) Off-resonance rotating-frame amide proton spin relaxation experiments measuring microsecond chemical exchange in proteins. J Biomol NMR 32:163–173
Lundström P, Vallurupalli P, Religa TL, Dahlquist FW, Kay LE (2007) A single-quantum methyl ^{13}C-relaxation dispersion experiment with improved sensitivity. J Biomol NMR 38:79–88
Lundström P, Hansen DF, Kay LE (2008) Measurement of carbonyl chemical shifts of excited protein states by relaxation dispersion NMR spectroscopy: comparison between uniformly and selectively ^{13}C labeled samples. J Biomol NMR 42:35–47
Lundström P, Hansen DF, Vallurupalli P, Kay LE (2009a) Accurate Measurement of alpha proton chemical shifts of excited protein states by relaxation dispersion NMR spectroscopy. J Am Chem Soc 131:1915–1926
Lundström P, Lin H, Kay LE (2009b) Measuring ^{13}Cβ chemical shifts of invisible excited states in proteins by relaxation dispersion NMR spectroscopy. J Biomol NMR 44:139–155
Malmendal A, Evenäs J, Forsén S, Akke M (1999) Structural dynamics in the C-terminal domain of calmodulin at low calcium levels. J Mol Biol 293:883–899
Massi F, Grey MJ, Palmer AG 3rd (2005) Microsecond timescale backbone conformational dynamics in ubiquitin studied with NMR $R_{1\rho}$ relaxation experiments. Protein Sci 14:735–742
Meiboom S, Gill D (1958) Modified spin-echo method for measuring nuclear spin relaxation times. Rev Sci Instrum 29:688–691
Mulder FAA, Akke M (2003) Carbonyl ^{13}C transverse relaxation measurements to sample protein backbone dynamics. Magn Reson Chem 41:853–865
Mulder FAA, Hon B, Muhandiram DR, Dahlquist FW, Kay LE (2000) Flexibility and ligand exchange in a buried cavity mutant of T4 lysozyme studied by multinuclear NMR. Biochemistry 39:12614–12622
Mulder FAA, Hon B, Mittermaier A, Dahlquist FW, Kay LE (2002) Slow internal dynamics in proteins: application of NMR relaxation dispersion spectroscopy to methyl groups in a cavity mutant of T4 lysozyme. J Am Chem Soc 124:1443–1451

Ollerenshaw JE, Tugarinov V, Skrynnikov NR, Kay LE (2005) Comparison of $^{13}CH_3$, $^{13}CH_2D$, and $^{13}CHD_2$ methyl labeling strategies in proteins. J Biomol NMR 33:25–41

Otten R, Chu B, Krewulak KD, Vogel HJ, Mulder FAA (2010a) Comprehensive and cost-effective NMR spectroscopy of methyl groups in large proteins. J Am Chem Soc 132:2952–2960

Otten R, Villali J, Kern D, Mulder FAA (2010b) Probing microsecond time scale dynamics in proteins by methyl ^{1}H Carr-Purcell-Meiboom-Gill relaxation dispersion NMR measurements. application to activation of the signaling protein NtrC(r). J Am Chem Soc 132:17004–17014

Paquin R, Ferrage F, Mulder FAA, Akke M, Bodenhausen G (2008) Multiple-timescale dynamics of side-chain carboxyl and carbonyl groups in proteins by ^{13}C nuclear spin relaxation. J Am Chem Soc 130:15805–15807

Press WH, Flannery BP, Teukolsky SA, Vetterling WT (1988) Numerical recipes in C. University Press, Cambridge

Schleucher J, Quant J, Glaser SJ, Griesinger C (1995) A theorem relating cross-relaxation and Hartmann–Hahn transfer in multiple-pulse sequences—optimal suppression of Tocsy transfer in Roesy. J Magn Reson Ser A 112:144–151

Skrynnikov NR, Mulder FAA, Hon B, Dahlquist FW, Kay LE (2001) Probing slow time scale dynamics at methyl-containing side chains in proteins by relaxation dispersion NMR measurements: application to methionine residues in a cavity mutant of T4 lysozyme. J Am Chem Soc 123:4556–4566

Sprangers R, Gribun A, Hwang PM, Houry WA, Kay LE (2005) Quantitative NMR spectroscopy of supramolecular complexes: dynamic side pores in ClpP are important for product release. P Natl Acad Sci USA 102:16678–16683

Ulrich EL, Akutsu H, Doreleijers JF, Harano Y, Ioannidis YE, Lin J, Livny M, Mading S, Maziuk D, Miller Z, Nakatani E, Schulte CF, Tolmie DE, Wenger RK, Yao HY, Markley JL (2008) BioMagResBank. Nucleic Acids Res 36:D402–D408

Vallurupalli P, Hansen DF, Stollar E, Meirovitch E, Kay LE (2007) Measurement of bond vector orientations in invisible excited states of proteins. P Natl Acad Sci USA 104:18473–18477

Vallurupalli P, Bouvignies G, Kay LE (2011) Increasing the exchange time-scale that can be probed by CPMG relaxation dispersion NMR. J Phys Chem B 115:14891–14900

Weininger U, Liu Z, McIntyre DD, Vogel HJ, Akke M (2012a) Specific $^{12}CbD_2^{12}CgD_2S^{13}CeHD_2$ isotopomer labeling of methionine to characterize protein dynamics by ^{1}H and ^{13}C NMR relaxation dispersion. J Am Chem Soc 134:18562–18565

Weininger U, Respondek M, Akke M (2012b) Conformational exchange of aromatic side chains characterized by L-optimized TROSY-selected ^{13}C CPMG relaxation dispersion. J Biomol NMR 54:9–14